Biochimie 98 (2014) 127–134

Contents lists available at ScienceDirect

Biochimie

journal homepage: www.elsevier.com/locate/biochi

Research paper

In vivo labeling of peroxisomes by photoconvertible mEos2 in myelinating glia of mice☆

Sarah Richert [a], Sandra Kleinecke [a], Jenniffer Günther [a], Florian Schaumburg [a], Julia Edgar [a], Gerd Ulrich Nienhaus [b], Klaus-Armin Nave [a], Celia M. Kassmann [a,*]

[a] Department of Neurogenetics, Max Planck Institute of Experimental Medicine, Hermann-Rein-Straße 3, 37075 Göttingen, Germany
[b] Institute of Applied Physics (APH) and Institute of Toxicology and Genetics (ITG), Karlsruhe Institute of Technology (KIT), Wolfgang-Gaede-Strasse 1, 76131 Karlsruhe, Germany

ARTICLE INFO

Article history:
Received 28 June 2013
Accepted 31 October 2013
Available online 18 November 2013

Keywords:
Transgenic mouse
Photoconversion
Fluorescent peroxisomes
Oligodendrocytes
mEos2

ABSTRACT

Mutations of several genes encoding peroxisomal proteins have been associated with human diseases. Some of these display specific white matter abnormalities in the brain, although the affected proteins are ubiquitously expressed. To better understand the etiology of peroxisomal myelin diseases, we aimed to label these organelles *in vivo* and in a cell type specific fashion. We had previously shown that in oligodendrocytes and Schwann cells numerous peroxisomes reside in the cytoplasmic channels of "non-compacted" myelin. These organelles are smaller and biochemically distinct from non-myelin peroxisomes. Targeting peroxisomal functions in various cell types of the brain has demonstrated that oligodendroglial peroxisomes are specifically important for long-term integrity of the CNS. To visualize myelin peroxisomes in intact cells and tissues by live imaging, we have generated a novel line of transgenic mice for the expression of fluorescently tagged peroxisomes specifically in myelinating glia. This was achieved by modifying the gene for a photoconvertible mEos2 with a peroxisomal targeting signal type 1 (PTS1) and generating a fusion gene with the myelin-specific *Cnp1* promoter. In the brain of resulting transgenic mice, peroxisomes are selectively labeled in oligodendrocytes. In this novel genetic tool, photoconversion of single peroxisomes from green to red fluorescence can be used to monitor the fate of single organelles and to determine the dynamics of PTS1-mediated protein import in the context of myelin diseases that affect peroxisomal functions.

1. Introduction

Peroxisomes are a group of heterogeneous organelles for compartmentalized anabolic and catabolic reactions, specifically in lipid metabolism [1]. Diversity of peroxisomes has been observed frequently in different tissues and suggests functional and cell type-specific specializations of this organelle, reflecting also different metabolic demands [2]. In the central nervous system (CNS) neuronal and glial cell types differ in the content of several peroxisomal proteins, including key enzymes such as catalase, D-aspartate oxidase, and acyl-CoA oxidase [3,4].

The most severe human peroxisomal disorder is the Zellweger syndrome (ZS) that is lethal in the postnatal period [5]. Underlying this heterogeneous group of disorders is usually a complete peroxisomal dysfunction caused by mutations in one of several essential peroxins (PEX). PEX proteins are involved in peroxisomal biogenesis, with PEX5 being a central participant in this process. This cytosolic cycling receptor is necessary for the import of globular proteins bearing a type 1 peroxisomal targeting signal (PTS1). The C-terminal tripeptide SKL is the prototype of a PTS1 [6]. Since

Abbreviations: AC, anterior commissure; ACAA1, acetyl-CoA acyltransferase; APP, amyloid precursor protein; bp, base pair; CB, cerebellar white matter; CC, corpus callosum; cDNA, complementary DNA; CTX, cerebral cortex; CNP, cyclic nucleotide phosphodiesterase; CNS, central nervous system; DNA, deoxyribonucleic acid; GFAP, glial fibrillary acidic protein; GFP, green fluorescent protein; HBSS, Hanks' balanced salt solution; HS, horse serum; Iba1, ionized calcium binding adaptor molecule 1; kb, kilobase; Lamp1, lysosomal associated membrane protein 1; LSM, laser scanning microscope; mEos2, monomeric fluorescent protein Eos 2; MRP-S21, mitochondrial ribosomal protein S21; NeuN, neuronal nuclear protein; Olig2, oligodendrocyte lineage transcription factor 2; OPC, oligodendrocyte precursor cell; P, postnatal day; PBS, phosphate buffered saline; PEX, peroxin; PMP70, peroxisomal membrane protein 70; PNS, peripheral nervous system; PCR, polymerase chain reaction; PTS1, peroxisomal targeting signal type 1; SV40 polyA, simian virus polyadenylation sequence; TUNEL, terminal deoxynucleotidyl transferase dUTP nick end labeling; WM, white matter; WT, wild-type; X-ALD, X-linked adrenoleukodystrophy; ZS, Zellweger syndrome.

* Corresponding author. Tel.: +49 551 3899 784; fax: +49 551 3899 753.
E-mail addresses: Richert@em.mpg.de (S. Richert), Kleinecke@em.mpg.de (S. Kleinecke), Barth@em.mpg.de (J. Günther), Schaumburg@em.mpg.de (F. Schaumburg), Edgar@em.mpg.de (J. Edgar), Uli.Nienhaus@kit.edu (G.U. Nienhaus), Nave@em.mpg.de (K.-A. Nave), Kassmann@em.mpg.de (C.M. Kassmann).

0300-9084/$ – see front matter © 2013 The Authors. Published by Elsevier Masson SAS. All rights reserved.
http://dx.doi.org/10.1016/j.biochi.2013.10.022

its discovery the SKL sequence has been successfully used in many systems to visualize peroxisomes in cultured cells. This was achieved by expression of fusion proteins harboring the SKL motif at the C-terminus of various reporter proteins [7,8]. Recently, a red fluorescent protein (mRuby) was reported, in which a related C-terminal sequence (GRL) emerged as a functional PTS that allowed visualizing peroxisomes in cultured cells [9].

The pronounced neurodegeneration seen in peroxisomal disorders has led to the extensive investigation of peroxisomal functions in the nervous system. Several mouse mutants were generated that lack either a PEX protein or another essential protein of specific peroxisomal functions [10–21]. More recently, cell type-specific ablation of most peroxisomal functions was achieved in various neural cell types [22–24]. This revealed a key function of oligodendroglial peroxisomes in maintaining myelin and axonal integrity of the CNS.

To enable the analysis of peroxisomes in myelinating cells *in vivo*, *ex vivo* and by live cell imaging of intact tissue and primary cultured cells, we have generated and characterized transgenic mice with fluorescently tagged peroxisomes. The myelin-specific *Cnp1* promoter was used to drive expression of the transgene in myelinating cells [25]. Peroxisomal targeting was achieved by fusion of C-terminal SKL to the coding sequence of photoconvertible mEos2 protein, a variant of EosFP [26,27].

2. Material and methods

2.1. Mouse genetics

A standardized fusion 3-step polymerase chain reaction (PCR) was performed using four primers, a *Cnp1* promoter plasmid, and a plasmid containing the coding sequence of mEos2 served as templates DNA (primer sequences are available upon request) [25]. The generated fragment contained 396 bp of the *Cnp1* promoter sequence downstream of the AflII restriction site and the complete coding sequence of mEos2. The antisense primer of mEos2 was designed such that 9 bp (encoding Ser, Lys, Leu for peroxisomal targeting) were inserted directly before the stop codon and a BamHI restriction site was added downstream of the stop codon. It was ligated into pGEM-T vector (Promega) for TA-cloning and by use of AflII and BamHI restriction sites cloned into the *Cnp1* promoter plasmid. Restriction sites, XbaI (upstream) and ClaI (downstream), flanked a 5.1 kb sequence including *Cnp1* promoter (3.9 kb) [28], mEos2 coding sequence with PTS1 (687 bp), and polyadenylation signal sequence of Simian virus 40 (120 bp). After restriction digest with XbaI and ClaI enzymes the DNA was purified by QIAquick spin columns (Qiagen). The linearized DNA was injected into C57BL/6N mouse oocytes according to standard procedures.

For genotyping, genomic DNA was isolated from tail biopsies using the DNeasy 96 tissue kit (Qiagen) according to the manufacturer's directions. Routine genotyping PCR was performed with sense (5′-CTTCTTACACAGGCCACCATGAGTGCG-3′) and antisense primers (5′-GGATCCTTACTTAGTTAAAGCTTGGATCGT-3′) yielding a 722 bp fragment, containing the mEos2 sequence.

Animal experiments were carried out in compliance with approved animal policies of the MPI of Experimental Medicine.

2.2. Histology

Mice were anesthetized with avertin (100 µl/10 g bodyweight) and perfused intracardially with HBSS (Lonza) followed by 4% paraformaldehyde (PFA) in 100 mM phosphate buffer. After dissection, brains were postfixed in the same fixative overnight. Sagittal vibratome sections of 40–50 µm were generated (Leica VT 1000S, Leica Instruments, Nussloch, Germany) and used for immunohistochemical stainings. Brain sections were permeabilized in 0.4% Triton in PBS for 30 min. Blocking was performed for 30 min in 4% Horse serum (HS) and 0.2% Triton in PBS. Primary antibody incubation was carried out overnight at 4 °C in 1% HS and 0.05% Triton in PBS. Incubation of fluorescently labeled secondary antibodies was carried out at room temperature for 2 h in 1.5% HS and sections were mounted in AquaPolymount (Polysciences, Warrington, PA).

Antibodies were used as follows: ACAA1 (ProteinTech Group) 1:200; GFAP (DAKO) 1:500; Iba1 (Wako) 1:1000; Lamp1 (PharMingen) 1:200; MRP-S21 (Antibodies-online) 1:50; NeuN (Millipore) 1:100; Olig2 (provided by J. Alberta [29]) 1:200; PMP70 (Abcam) 1:600; PMP70 (Sigma–Aldrich) 1:400, and secondary fluorescence-conjugated Alexa-488, Alexa-555 (1:2000, Invitrogen) or DyLight 633 (1:200, YO Proteins).

2.3. Cell culture

Oli-neu cells, an oligodendroglial precursor cell line, were obtained from Jacqueline Trotter (university of Mainz). Cultivation and electroporation of cells was performed as described earlier [30,31].

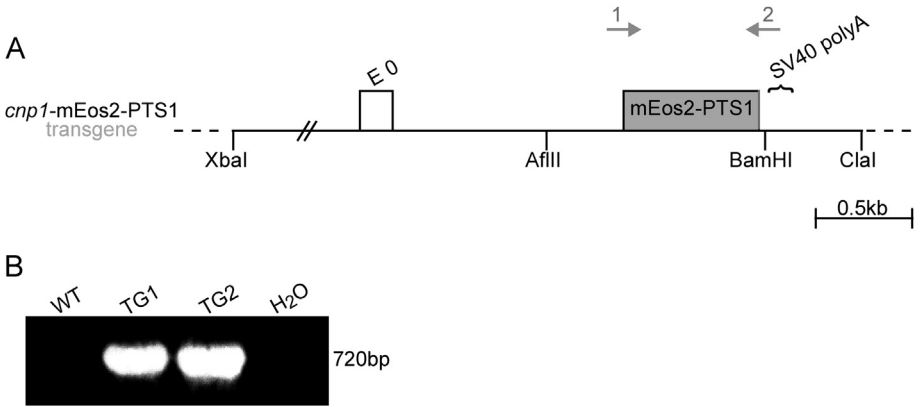

Fig. 1. Identification of genomic transgene insertion and of mEos2 expression in mice. (A) Structure of the *Cnp-mEos2-PTS1* transgene containing 3.9 kb of the CNP1 promoter and the mEos2 coding sequence cloned into the original start codon of CNP1. 9 extra base pairs are inserted upstream adjacent to the stop codon, encoding three amino acids (Ser, Lys and Leu), a type 1 peroxisomal targeting signal (PTS1). Downstream the sequence is flanked by a polyadenylation signal sequence of the Simian virus 40 (SV40 polyA). E0 indicates exon 0 of the *CNP* gene. (B) Genotyping PCR by use of primers 1 and 2 showing a fragment of the expected size when template DNA was obtained from transgenic animals (TG) but not from wild-type controls (WT).

Mouse embryonic fibroblasts were generated from wild-type mouse embryos at embryonic day 14.5 (E14.5) according to standard procedures described elsewhere [32]. Fibroblasts for live cell imaging were seeded and imaged in μ-dish cell culture imaging dishes (Ibidi, Germany) coated with poly-L-lysin. Transfection with mEos2-PTS1 construct (in the pEGFP-N1 vector, Clonetech) was carried out with Lipofectamin2000 (Invitrogen) according to manufacturer's directions. Cells were cultured in a humidified incubator (5% CO_2 at 37 °C). For imaging cells were transferred to a temperature and CO_2 controlled microscope incubation chamber.

2.4. Imaging and image processing

Fluorescent images were acquired with an inverted Zeiss Axio Observer. For green fluorescence mEos2-PTS1 signal was excited using a 426–446 nm bandpass filter, and emission was recorded with a 520–550 nm bandpass filter. For red fluorescence a 535–557 nm bandpass filter was used, and emission was recorded with a 570–640 nm bandpass filter. Conversion of mEos2-PTS1 protein was carried out with excitation Filter G 365, illuminating for 1 s when using a 63× objective. 10 s of illumination were required for photoconversion using a 10× objective.

Images were processed with ImageJ software, version 1.47u. Co-localization of Olig2-positive nuclei and perinuclear mEos2 signal was measured with Imaris software, version 7.52 (Bitplane AG, Switzerland) and calculations were performed with GraphPad Prism 5.

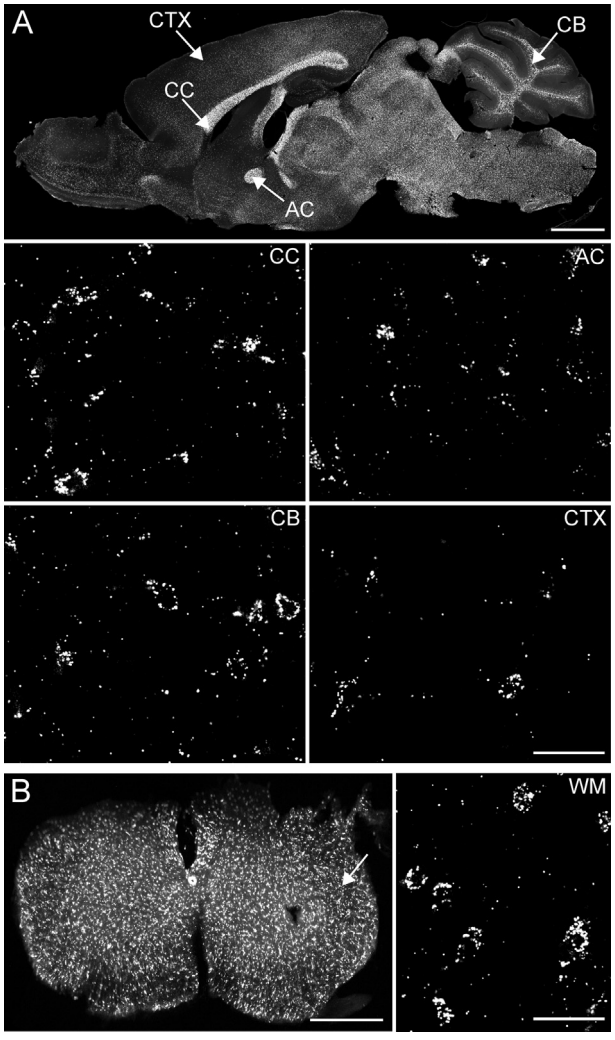

Fig. 2. mEos2 expression in the brain of *Cnp-mEos2-PTS1* transgenic mice. (A) Sagittal vibratome brain section of a transgenic mouse at 2 months displays high expression of the transgene particularly in white matter structures. Scale bar, 1.5 mm. Middle and bottom panels show magnifications of the corpus callosum (CC), the anterior commissure (AC), cerebellar white matter (CB), and the cerebral cortex (CTX). Scale bars, 20 μm. (B) Expression is also abundant in the spinal cord as visualized by fluorescence of a spinal cord cross-section (left; Scale bar, 0.5 mm) and magnification of spinal cord white matter (WM; right). Scale bar, 20 μm.

3. Results

3.1. Generation of transgenic mice

A fusion polymerase chain reaction (PCR) was performed to generate a 1.1 kb mEos2 cDNA fragment terminated by restriction sites suitable for subsequent cloning (Fig. 1A). This fragment contained the coding sequence of mEos2 with a 9 bp 3′ extension encoding the SKL peroxisomal targeting signal (PTS1). The fragment was inserted into a plasmid with the promoter of the 2′, 3′-cyclic nucleotide phosphodiesterase gene (*Cnp1*). To prevent mitochondrial targeting, we removed a 57 bp fragment upstream of the start codon for the CNP1 isoform, thereby eliminating the N-terminal mitochondrial targeting sequence of the CNP2 isoform [33]. Downstream the transgene was flanked by the SV40 polyadenylation signal (Fig. 1A). After injection of the linearized fragment into fertilized C57BL/6N oocytes, we obtained five potential founders (F0) from twenty-two mice, as assessed by PCR analysis (Fig. 1B). Transgenic animals were born at the expected Mendelian frequency and showed no obvious differences from wild-type littermates. Two lines were expanded and characterized in more detail. In the following, we concentrate on one line of *Cnp-mEos2-PTS1* mice that was optimally suited for studying myelin-associated peroxisomes.

3.2. Spatio-temporal expression pattern of Cnp-mEos2-PTS1

Fluorescence microscopic analysis of vibratome sections demonstrated high expression of mEos2 in the adult central nervous system, with pronounced localization of labeled peroxisomes in white matter tracts, such as corpus callosum, anterior commissure, and cerebellar white matter (Fig. 2). With respect to expression level, we noted a gradient most evident on sagittal sections with mEos2 expression stronger in caudal regions than in rostral regions (Fig. 2A). However, no region of brain and spinal cord was free of labeled peroxisomes (Fig. 2B). Similar to the developmental expression of CNP and other myelin proteins, mEos2+ puncta were readily detectable in spinal cord and in brain stem at postnatal day 7 (P7), and only later in frontal brain areas (data not shown) [34]. After P14 the expression pattern of mEos2 mice was essentially the same as in the CNS of adult transgenic mice. However, at this early stage the expression level was lower than in older mice, which maintained the adult expression levels as visualized by fluorescence intensity for at least 6 months (data not shown).

As expected, double-staining for the oligodendroglial transcription factor Olig2, revealed that the majority of cells in the oligodendroglial lineage were mEos2 positive (Fig. 3A). Most of this signal was punctate and perinuclear, but single mEos2+ puncta were also frequent deep in the glial cell processes. These puncta are most likely equivalent to single peroxisomes residing in "myelinic channels", such as the cytoplasm of non-compacted myelin at the adaxonal inner mesaxon [35].

Next, we quantified Olig2-positive nuclei that were associated with perinuclear mEos2 signal. All measured CNS regions (cerebellar white matter, anterior commissure, corpus callosum, and

cerebral cortex) showed a marked (60–80%) co-localization of Olig2 and mEos2 in the same oligodendrocyte lineage cells (Fig. 3B). In contrast, we never observed perinuclear mEos2 signals in GFAP-positive astrocytes, in Iba1-positive microglia/macrophages, or in NeuN-positive neurons (Suppl. Fig. 1). Taken together, these data suggest that we have achieved cell-specific expression of mEos2 by oligodendroglial cells (and some of their precursors) in the CNS of *Cnp-mEos2-PTS1* mice.

In contrast, teased fiber preparations of the sciatic nerve showed an extremely weak mEos2-signal (data not shown). This is consistent with the very low expression level of CNP in myelinating Schwann cells of the PNS [36]. Several other tissues tested, including heart, lung, liver, kidney, and muscle, did not reveal any fluorescent signal in *Cnp-mEos2-PTS1* transgenic mice (data not shown). However, we noted robust mEos2-expression in some cells of spleen and testis (Suppl. Fig. 2), in agreement with published data on enzymatic activity of CNP or immune staining of CNP [37,38]. Although, we did not perform co-localization studies with peroxisomal marker proteins in these tissues, the punctate signal in these tissues indicated targeting of peroxisomes.

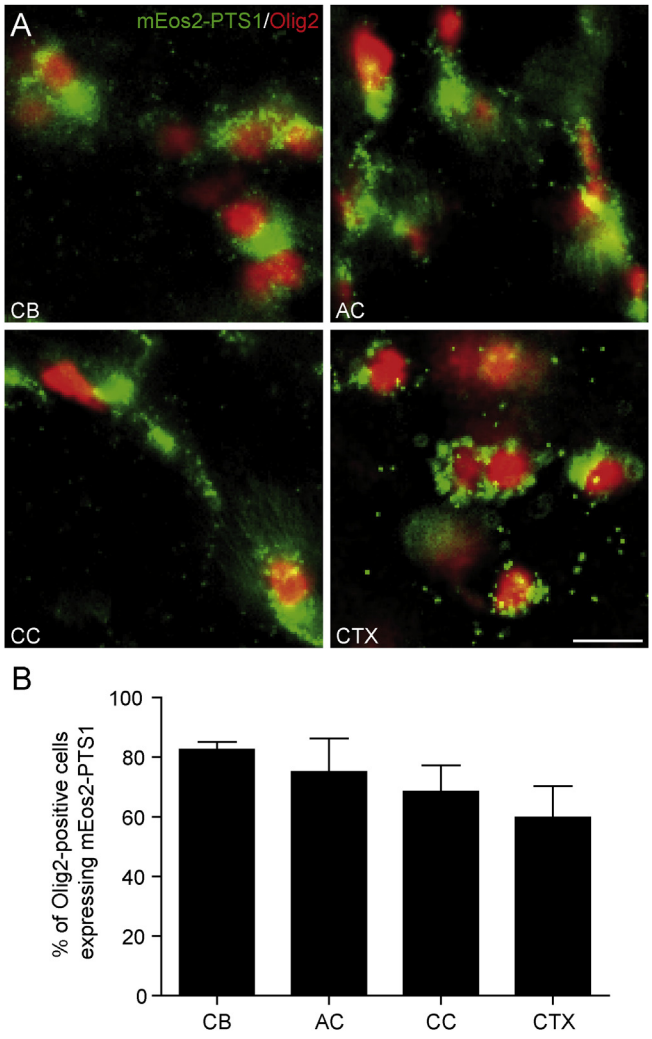

Fig. 3. mEos2 expression by Olig2-positive brain cells in *Cnp-mEos2-PTS1* transgenic mice. (A) Vibratome brain sections immune-stained for nuclear oligodendroglial maker protein Olig2 (red) shows high association of oligodendroglial cells with mEos2 fluorescence (green). Scale bar, 10 μm. (B) Graphic illustration of the high amount (≥60%) of Olig2-positive cells that express mEos2. It was quantified in different white matter regions (cerebellar white matter, CB; anterior commissure, AC; corpus callosum, CC) and in the cortex (CTX). Values are expressed as mean percentage ± SD; $n = 3$.

3.3. Peroxisomal targeting

To assess whether the fluorophore is exclusively targeted to peroxisomes *in vivo*, we performed subcellular co-localization studies on brain vibratome sections from transgenic mice (Fig. 4). Antibodies recognizing peroxisomal membrane protein 70 (PMP70) and peroxisomal acetyl-CoA acyltransferase 1 (ACAA1) confirmed targeting and localization of mEos2 in peroxisomes (Fig. 4A, B). To assess any additional targeting of the fusion protein to other organelles, we visualized mitochondria by co-staining of the mitochondrial ribosomal protein S21 (MRP-S21). This showed that mEos2 was never targeted to mitochondria (Fig. 4C). Also, the lysosome-associated membrane protein 1 (Lamp1), was never co-localized with mEos2 (Fig. 4D). Thus, by these criteria targeting of mEos2-PTS1 is specific to the peroxisomal compartment.

3.4. Photoconversion of mEos2

mEos2 was designed such that exposure to UV light converts the original green fluorescence (max. at 519 nm) into emission of red light (max. at 584 nm) [27]. However, the maxima of emission and excitation are dependent on the local pH, which is different in peroxisomes and cytoplasm [39,40]. We therefore investigated the

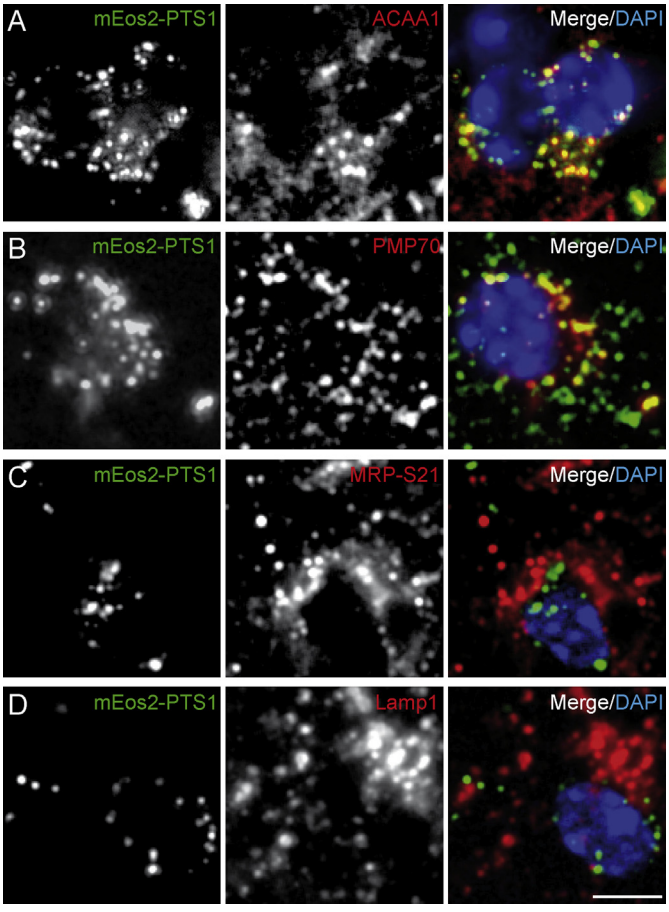

Fig. 4. Exclusive peroxisomal targeting of mEos2-PTS1 *in vivo*. Depicted are fluorescence micrographs of a transgenic mouse brain cortex. (A, B) mEos2-PTS1 (green) shows co-localization with the peroxisomal enzyme acetyl-CoA acyltransferase (ACAA1; red) and with peroxisomal membrane protein 70 (PMP70; red). (C, D) In contrast, no co-localization is observed with mitochondrial ribosomal protein S21 (MRP-S21; red) or with lysosome associated protein 1 (Lamp1; red). DAPI-stained nuclei are shown in blue (right). Scale bar, 5 μm.

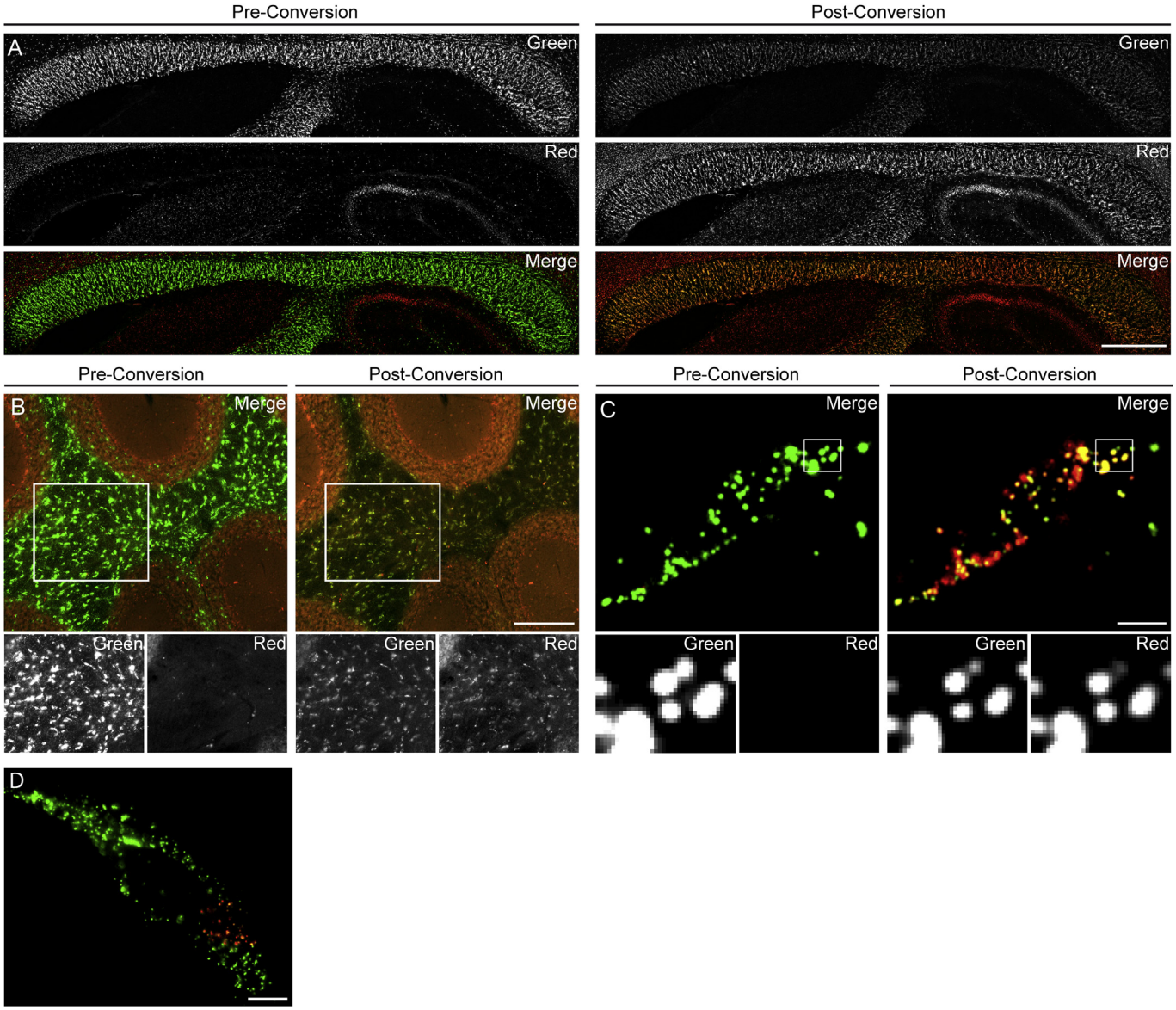

Fig. 5. Photoconversion of mEos2 in the transgenic mouse brain and in primary cells. Before irradiation with UV light, fluorescence of the fluorophore is strong in the green emission range, but almost absent in the red spectrum (left). Green fluorescence is reduced in favor of red fluorescence after photoconversion (right). (A) Corpus callosum (scale bar, 200 μm) and (B) cerebellum (scale bar, 200 μm) are shown. Insets magnify cerebellar white matter. (C) Photoconversion is demonstrated on single cell level in the corpus callosum with insets to enable visualization of single organelles. Scale bar, 5 μm. (D) Fluorescence within a rectangular region of interest of a transfected mouse fibroblast was switched to demonstrate photoconversion of single peroxisomes. Scale bar, 10 μm.

emission and excitation spectra of mEos2 inside peroxisomes of live cells.

We transfected oli-neu cells, a well-established oligodendroglial cell line [30] with the same DNA construct that was used for the generation of *Cnp-mEos2-PTS1* mice. After 2 days, we performed "lambda scans" with excitation between 470 nm and 670 nm and a step-width of 10 nm to measure the emission spectrum using a confocal laser-scanning microscope (LSM; data not shown). Next, we adapted a protocol for photoconversion of mEos2-PTS1 in PFA-fixed (and unfixed) brain sections, using a wide-field fluorescence microscope (Fig. 5). The switch from green to red emission was achieved after irradiation with UV light (340–390 nm) in all brain areas, including corpus callosum and cerebellar white matter (Fig. 5A, B). The converted fluorescence of single peroxisomes was readily evident by a magnified view of oligodendrocytes in the corpus callosum (Fig. 5C).

We also attempted to convert the fluorescence of only a subset of peroxisomes within a single cell. To this end mEos2-PTS1 transfected primary mouse fibroblasts were investigated using an inverted fluorescence microscope equipped for live cell imaging (Suppl. Video 1). A subcellular region of interest was irradiated with UV light using a rectangular diaphragm resulting in discrete number of peroxisomes with red fluorescence, while the majority of organelles exhibited green fluorescence (Fig. 5D).

Supplementary data related to this article can be found online at http://dx.doi.org/10.1016/j.biochi.2013.10.022.

3.5. *mEos2-PTS1 expression in oligodendrocytes is not toxic*

To analyze possible toxic effects of transgene expression in the brains of 12 months old mice, we searched for condensed nuclei (indicative of apoptosis) that are visible by H&E staining.

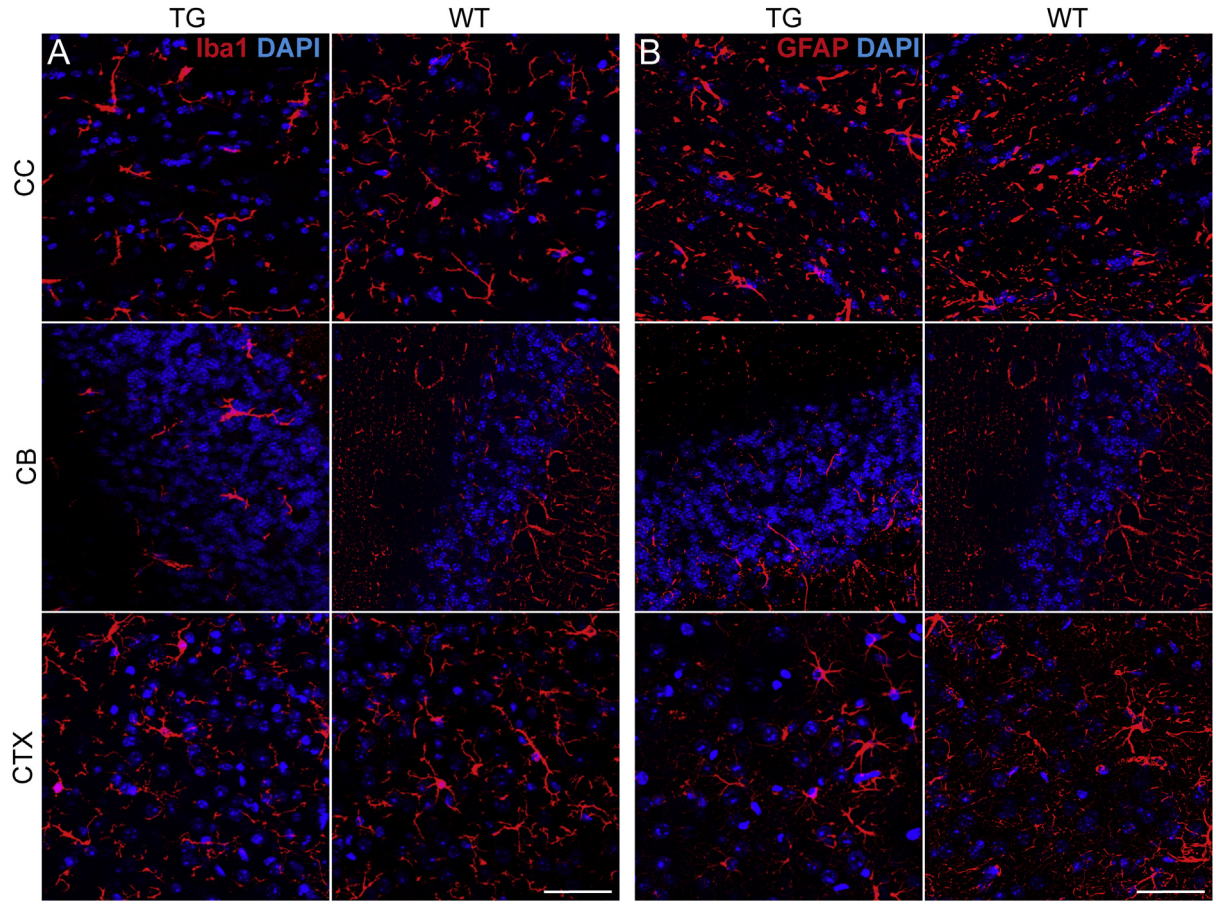

Fig. 6. Absence of reactive gliosis in the brain of transgenic mice aged 12 months. Immune-staining for (A) microglial Iba 1 and (B) astroglial glial fibrillary acidic protein (GFAP) do not show differences regarding expression level, morphology, or distribution of glial cells in the corpus callosum (top), the cerebellum (middle), and in the cortex (bottom) of transgenic mice. Scale bars, 50 μm.

In addition we used the terminal transferase dUTP nick end labeling (TUNEL) technique to mark nuclei with fragmented DNA. By either method, we found no difference between transgenic and wild-type mice in the frequency of apoptotic cells. We also obtained no evidence for axonal perturbations, such as amyloid precursor protein (APP)-positive swellings that are a feature of peroxisomal mutants (data not shown) [22]. When studying the brains of 12 months mice by immunohistochemistry, there was no difference in the distribution, density and morphology of astrocytes and microglial cells (Fig. 6). Up to one year of age we did not notice any sign of abnormal cage behavior (not shown). Taken together, this suggests that *Cnp-mEos2-PTS1* transgenic mice will be an useful tool to visualize peroxisomes in combination with neurological disease genes.

4. Discussion

The generation of mice with fluorescently labeled peroxisomes in oligodendrocytes was achieved with the myelin-specific *Cnp1* promoter that drives expression of mEos2 in oligodendrocytes. Fusion of the tripeptide SKL (a type 1 peroxisomal targeting signal; PTS1) at the C-terminus of the mEos2 protein has efficiently and exclusively mediated the targeting of the fluorophore into peroxisomes *in vivo*. We could show that transgene expression in the central nervous system of these mice is restricted to oligodendrocyte lineage cells. Independent of the CNS region analyzed, between approximately 60–80% of all oligodendrocyte lineage cells were positive for the fluorophore (but not 100%, see below). The expression was particularly high in white matter tracts, but also present in the majority of gray matter oligodendrocytes. Since the fluorescence was already detectable in many regions at age P7 and the final expression pattern was established by P14, these transgenic mice appear suitable for many developmental studies. Specifically, the analysis of peroxisomes in the CNS of adult and aged mice and in the context of neurodegenerative diseases will be possible, because there is no obvious toxicity of transgene expression at all ages studied (up to 12 months).

We defined oligodendrocyte lineage cells by the expression of Olig2 as a marker, which also stains oligodendrocyte precursor cells (OPC) prominently. The *Cnp1* promoter is active in mature oligodendrocytes, but only in 50% of adult OPC (Saab et al., in preparation). This suggests that virtually all mature oligodendrocytes express the *Cnp1*-driven transgene, as expected from similar transgenic studies [41]. However due to the low expression level of the *Cnp1* promoter in Schwann cells, these mice may be less suited for PNS analyses.

An advantage of mEos2 over other GFP-like reporter proteins is the convertible fluorescence changing the emission from the green to the red spectrum of light. We have shown that mEos2 fluorescence can be switched within a small region of interest to target only a subset of peroxisomes within a cell. It is theoretically possible to switch the fluorescence of only a single peroxisome in the process of an oligodendrocyte or within a myelin internode,

where the density of organelles is sufficiently low. This will enable us to follow the fate of single organelles by live imaging. Another application of the photoconvertible properties of mEos2 will be a monitoring of the rate of peroxisomal biogenesis and the fate of this organelle, similar to a "pulse-chase" experiment. When all resident peroxisomes are simultaneously switched to red, the appearance of newly formed (green) peroxisomes can be easily monitored and the half-live of (red) peroxisomes and their elimination by autophagy can be quantified.

Ligands of peroxisome proliferator-activated receptors (PPARs) are able to induce peroxisome proliferation and possibly biogenesis in liver cells [42,43], but little is known about similar effects on oligodendrocytes in which peroxisomes serve a neuroprotective function [22]. The *Cnp-mEos2-PTS1* transgenic mouse will enable us to explore PPAR signaling and other drug effects on peroxisome biogenesis and turnover in the brain. Similarly, the rate of peroxisomal protein import can be determined *in situ*, which is of relevance for specific peroxisomal defects, such as in X-linked adrenoleukodystrophy, a disease that has been suspected to reflect secondary organelle dysfunctions [22,44].

Acknowledgments

We are grateful to "Olivers Army" (England) and "The Myelin Project" (USA/Germany) for the generous support of this project. We thank J. Rietdorf (Zeiss, Munich, Germany), F. Kirchhoff (University of Homburg/Saar, Germany), and M. Rossner for helpful discussions. We also thank U. Fünfschilling, R. Libal and A. Kanbach for support in the generation of transgenic mice. J.E. is supported by an ERC Advanced Grant to K.A.N.

Appendix A. Supplementary data

Supplementary data related to this article can be found at http://dx.doi.org/10.1016/j.biochi.2013.10.022.

References

[1] R.J.A. Wanders, H.R. Waterham, Biochemistry of mammalian peroxisomes revisited, Annu. Rev. Biochem. 75 (2006) 295–332.
[2] M. Fransen, Peroxisome dynamics: molecular players, mechanisms, and (Dys) functions, ISRN Cell Biol. 2012 (2012) 1–24.
[3] K. Zaar, H.-P. Köst, A. Schad, A. Völkl, E. Baumgart, H.D. Fahimi, Cellular and subcellular distribution of D-aspartate oxidase in human and rat brain, J. Comp. Neurol. 450 (2002) 272–282.
[4] B. Ahlemeyer, I. Neubert, W.J. Kovacs, E. Baumgart-Vogt, Differential expression of peroxisomal matrix and membrane proteins during postnatal development of mouse brain, J. Comp. Neurol. 505 (2007) 1–17.
[5] N.E. Braverman, M.D. D'Agostino, G.E. MacLean, Peroxisome biogenesis disorders: Biological, clinical and pathophysiological perspectives, Dev. Disabil. Res. Rev. 17 (2013) 187–196.
[6] S.J.S. Gould, G.A.G. Keller, N.N. Hosken, J.J. Wilkinson, S.S. Subramani, A conserved tripeptide sorts proteins to peroxisomes, J. Cell Biol. 108 (1989) 1657–1664.
[7] H.J. Kim, I.S. Woo, E.S. Kang, S.Y. Eun, H.J. Kim, J.H. Lee, et al., Identification of a truncated alternative splicing variant of human PPARgamma1 that exhibits dominant negative activity, Biochem. Biophys. Res. Commun. 347 (2006) 698–706.
[8] O. Ivashchenko, P.P. Van Veldhoven, C. Brees, Ye-Shih Ho, S.R. Terlecky, M. Fransen, Intraperoxisomal redox balance in mammalian cells: oxidative stress and interorganellar cross-talk, Mol. Biol. Cell 22 (2011) 1440–1451.
[9] S. Kredel, F. Oswald, K. Nienhaus, K. Deuschle, C. Röcker, M. Wolff, et al., mRuby, a bright monomeric red fluorescent protein for labeling of subcellular structures, PLoS One 4 (2009) e4391.
[10] C.Y. Fan, J. Pan, R. Chu, D. Lee, K.D. Kluckman, N. Usuda, et al., Targeted disruption of the peroxisomal fatty acyl-CoA oxidase gene: generation of a mouse model of pseudoneonatal adrenoleukodystrophy, Ann. N. Y. Acad. Sci. 804 (1996) 530–541.
[11] M. Baes, P. Gressens, E. Baumgart, P. Carmeliet, M. Casteels, M. Fransen, et al., A mouse model for Zellweger syndrome, Nat. Genet. 17 (1997) 49–57.
[12] P.L. Faust, M.E. Hatten, Targeted deletion of the PEX2 peroxisome assembly gene in mice provides a model for Zellweger syndrome, a human neuronal migration disorder, J. Cell Biol. 139 (1997) 1293–1305.
[13] S. Forss-Petter, H. Werner, J. Berger, H. Lassmann, B. Molzer, M.H. Schwab, et al., Targeted inactivation of the X-linked adrenoleukodystrophy gene in mice, J. Neurosci. Res. 50 (1997) 829–843.
[14] Kobayashi, N. Shinnoh, A. Kondo, T. Yamada, Adrenoleukodystrophy protein-deficient mice represent abnormality of very long chain fatty acid metabolism, Biochem. Biophys. Res. Commun. 232 (1997) 631–636.
[15] J.F. Lu, A.M. Lawler, P.A. Watkins, J.M. Powers, A.B. Moser, H.W. Moser, et al., A mouse model for X-linked adrenoleukodystrophy, Proc. Natl. Acad. Sci. U. S. A. 94 (1997) 9366–9371.
[16] P. Brites, A.M. Motley, P. Gressens, P.A.W. Mooyer, I. Ploegaert, V. Everts, et al., Impaired neuronal migration and endochondral ossification in Pex7 knockout mice: a model for rhizomelic chondrodysplasia punctata, Hum. Mol. Genet. 12 (2003) 2255–2267.
[17] Y.-S. Ho, Y. Xiong, W. Ma, A. Spector, D.S. Ho, Mice lacking catalase develop normally but show differential sensitivity to oxidant tissue injury, J. Biol. Chem. 279 (2004) 32804–32812.
[18] G. Chevillard, M.-C. Clémencet, N. Latruffe, V. Nicolas-Francès, Targeted disruption of the peroxisomal thiolase B gene in mouse: a new model to study disorders related to peroxisomal lipid metabolism, Biochimie 86 (2004) 849–856.
[19] S. Ferdinandusse, S. Denis, H. Overmars, L. Van Eeckhoudt, P.P. Van Veldhoven, M. Duran, et al., Developmental changes of bile acid composition and conjugation in L- and D-bifunctional protein single and double knockout mice, J. Biol. Chem. 280 (2005) 18658–18666.
[20] I. Ferrer, J.P. Kapfhammer, C. Hindelang, S. Kemp, N. Troffer-Charlier, V. Broccoli, et al., Inactivation of the peroxisomal ABCD2 transporter in the mouse leads to late-onset ataxia involving mitochondria, Golgi and endoplasmic reticulum damage, Hum. Mol. Genet. 14 (2005) 3565–3577.
[21] A. Teigler, D. Komljenovic, A. Draguhn, K. Gorgas, W.W. Just, Defects in myelination, paranode organization and Purkinje cell innervation in the ether lipid-deficient mouse cerebellum, Hum. Mol. Genet. 18 (2009) 1897–1908.
[22] C.M. Kassmann, C. Lappe-Siefke, M. Baes, B. Brügger, A. Mildner, H.B. Werner, et al., Axonal loss and neuroinflammation caused by peroxisome-deficient oligodendrocytes, Nat. Genet. 39 (2007) 969–976.
[23] L. Hulshagen, O. Krysko, A. Bottelbergs, S. Huyghe, R. Klein, P.P. Van Veldhoven, et al., Absence of functional peroxisomes from mouse CNS causes dysmyelination and axon degeneration, J. Neurosci. 28 (2008) 4015–4027.
[24] A. Bottelbergs, S. Verheijden, L. Hulshagen, D.H. Gutmann, S. Goebbels, K.-A. Nave, et al., Axonal integrity in the absence of functional peroxisomes from projection neurons and astrocytes, Glia 58 (2010) 1532–1543.
[25] C. Lappe-Siefke, S. Goebbels, M. Gravel, E. Nicksch, J. Lee, P.E. Braun, et al., Disruption of Cnp1 uncouples oligodendroglial functions in axonal support and myelination, Nat. Genet. 33 (2003) 366–374.
[26] J. Wiedenmann, EosFP, a fluorescent marker protein with UV-inducible green-to-red fluorescence conversion, Proc. Natl. Acad. Sci. U. S. A. 101 (2004) 15905–15910.
[27] S.A. McKinney, C.S. Murphy, K.L. Hazelwood, M.W. Davidson, L.L. Looger, A bright and photostable photoconvertible fluorescent protein, Nat. Meth. 6 (2009) 131–133.
[28] M. Gravel, A. Di Polo, P.B. Valera, P.E. Braun, Four-kilobase sequence of the mouse CNP gene directs spatial and temporal expression of lacZ in transgenic mice, J. Neurosci. Res. 53 (1998) 393–404.
[29] K.L. Ligon, J.A. Alberta, A.T. Kho, J. Weiss, M.R. Kwaan, C.L. Nutt, et al., The oligodendroglial lineage marker OLIG2 is universally expressed in diffuse gliomas, J. Neuropathol. Exp. Neurol. 63 (2004) 499–509.
[30] M. Jung, E. Krämer, M. Grzenkowski, K. Tang, W. Blakemore, A. Aguzzi, et al., Lines of murine oligodendroglial precursor cells immortalized by an activated neu tyrosine kinase show distinct degrees of interaction with axons in vitro and in vivo, Eur. J. Neurosci. 7 (1995) 1245–1265.
[31] C. Klein, E.-M. Kramer, A.-M. Cardine, B. Schraven, R. Brandt, J. Trotter, Process outgrowth of oligodendrocytes is promoted by interaction of fyn kinase with the cytoskeletal protein tau, J. Neurosci. 22 (2002) 698–707.
[32] J. Xu, Preparation, Culture, and Immortalization of Mouse Embryonic Fibroblasts, John Wiley & Sons, Inc, Hoboken, NJ, USA, 2001.
[33] J. Lee, R.C. O'Neill, M.W. Park, M. Gravel, P.E. Braun, Mitochondrial localization of CNP2 is regulated by phosphorylation of the N-terminal targeting signal by PKC: implications of a mitochondrial function for CNP2 in glial and non-glial cells, Mol. Cell. Neurosci. 31 (2006) 446–462.
[34] W.-P. Yu, E.J. Coliarini, N.P. Pringle, W.D. Richardson, Embryonic expression of myelin genes: evidence for a focal source of oligodendrocyte precursors in the ventricular zone of the neural tube, Neuron 12 (1994) 1353–1362.
[35] C.M. Kassmann, S. Quintes, J. Rietdorf, W. Möbius, M.W. Sereda, T. Nientiedt, et al., A role for myelin-associated peroxisomes in maintaining paranodal loops and axonal integrity, FEBS Lett. 585 (2011) 2205–2211.
[36] T.J. Sprinkle, F.A. McMorris, J. Yoshino, G.H. DeVries, Differential expression of 2′:3′-cyclic nucleotide 3′-phosphodiesterase in cultured central, peripheral, and extraneural cells, Neurochem. Res. 10 (1985) 919–931.
[37] S. Weissbarth, H.S. Maker, I. Raes, T.S. Brannan, E.P. Lapin, G.M. Lehrer, The activity of 2′,3′-cyclic nucleotide 3′-phosphodiesterase in rat tissues, J. Neurochem. 37 (1981) 677–680.
[38] M.S. Davidoff, R. Middendorff, E. Köfüncü, D. Müller, D. Jezek, A.F. Holstein, Leydig cells of the human testis possess astrocyte and oligodendrocyte marker molecules, Acta Histochem. 104 (2002) 39–49.

[39] T.B. Dansen, K.W. Wirtz, R.J. Wanders, E.H. Pap, Peroxisomes in human fibroblasts have a basic pH, Nat. Cell Biol. 2 (2000) 51–53.
[40] M. Kneen, J. Farinas, Y. Li, A.S. Verkman, Green fluorescent protein as a noninvasive intracellular pH indicator, Biophysical. J. 74 (1998) 1591–1599.
[41] S. Belachew, X. Yuan, V. Gallo, Unraveling oligodendrocyte origin and function by cell-specific transgenesis, Dev. Neurosci. 23 (2001) 287–298.
[42] M. Schrader, H.D. Fahimi, Growth and division of peroxisomes, Int. Rev. Cytol. 255 (2006) 237–290.
[43] M. Schrader, N.A. Bonekamp, M. Islinger, Fission and proliferation of peroxisomes, Biochim. Biophys. Acta 1822 (2012) 1343–1357.
[44] I. Singh, A. Pujol, Pathomechanisms underlying X-adrenoleukodystrophy: a three-hit hypothesis, Brain Pathol. 20 (2010) 838–844.s.